Theoretical Study of the Double Proton Transfer in Hydrogen-Bonded Complexes in the Gas Phase and in Solution: Prototropic Tautomerization of Formamide

Yangsoo Kim, Sangbae Lim, Hyun-Jin Kim, and Yongho Kim*

Department of Chemistry, Kyung Hee University, Yongin-City, Kyunggi-Do, 449-701, Korea

Received: September 8, 1998

Double proton transfers in the prototropic tautomerism of formamide dimer and monohydrated formamide in the gas phase and in solution have been studied as prototypes of multiple proton transfer. The potential energy surface (PES) for the double proton transfer was studied using ab initio quantum mechanical methods, and the solvent effect on the PES was included using the self-consistent reaction field model. In the gas phase, the transition state for the double proton transfer in formamide dimer has C_s symmetry, when the Hartree−Fock (HF) level of theory is used. When the MP2 and B3LYP levels of theory are used to consider electron correlation, the transition state has C_{2h} symmetry. The double proton transfer occurs concertedly and synchronously. The H bonds in homodimers are stronger than in monohydrated complexes, and the H bonds with formamidic acid are stronger than with formamide. The changes in the H-bond strengths and distances were also calculated as the dielectric constant was increased. The barrier height depends very much on the electron correlation, and the reaction energies of the tautomerization are very sensitive to the size of basis sets. The potential energy barrier for the tautomerization is lowered about 30 kcal mol^{-1} in the gas phase by forming hydrogen-bonded dimer. The dimer-assisted tautomerization is kinetically more favorable, but thermodynamically less favorable, than the water-assisted. The tautomerization energies and the potential energy barriers are increased as the dielectric constant is increased both for the water-assisted and for the dimer-assisted reactions, which imply that the tautomerization of formamide becomes less favorable in a polar solvent.

Introduction

Proton transfer is one of the simplest and the most fundamental reaction in chemistry and is important in oxidation−reduction reactions in many chemical and biological reactions.[1−3] Proton transfer over a long distance involving many protons is also an important phenomenon in chemistry and biology. Most long-range multiproton transfers occur, either synchronously or asynchronously, through a hydrogen-bonded chain. There are many examples of multiproton transfer such as proton relay systems in enzymes, certain proton transfers in hydrogen-bonded water complexes, and proton transfers in prototropic tautomerisms. A proton relay is thought to account for the high mobility of the proton in water. Double proton transfer occurs in DNA base pair such as the adenine−thymine base pair. Limbach et al. have studied the double proton transfer in prototropic tautomerisms for many amidine systems and porphyrins using the dynamic NMR technique.[4−8] They reported rates and the kinetic isotope effects for both concerted and stepwise double proton transfers. Formic acid dimer is one of the most extensively studied systems both experimentally and theoretically,[9−15] since it is one of the simplest examples of a multiproton transfer system in which the constituents are held together by two hydrogen bonds. Therefore, it can be used as a model of many chemically and biologically important multiproton transfers. In addition to serving as a model for hydrogen transfer reactions in bases of nucleic acids, formamidine has been extensively studied theoretically since it also forms homodimers and hydrogen bonds with water. Intramolecular and intermolecular hydrogen transfers have been studied theoretically for various formamidine systems.[5,6,16−19] Proton transfers in formamidine dimer can also be considered a prototype of multiproton transfer. They can also provide information about hydrogen bonding, as well as the proton relay mechanism in enzymes. Recently, the dynamics of double proton transfer in formic acid dimer[15] and monohydrated formamidine[20,21] have been studied in the gas phase. The solvent effect on the potential energy surface for the double proton transfer in formic acid dimer and formamidine dimer has also been studied.[22]

The prototropic tautomerization of formamide has recently been studied by several workers since it is important in proteins and can be used as a model for tautomerization in nucleic acid bases.[23,24] Most of the theoretical studies have focused on the geometric change, relative stability of tautomers, and the energetic stabilization due to the hydrogen bonds in the gas phase.[23,25] Since most proton transfers occur in aqueous solution, one must consider the role of water molecules in the proton transfer. Water can act not only as a solvent but also as a mediator which gives or accepts protons to promote the long-range proton transfer. Simons and co-workers[24] have recently shown that the potential energy barrier for the tautomerization of formamide is lowered about 26 kcal mol^{-1} by adding a single H_2O molecule. Because of the light mass of the proton, quantum mechanical tunneling is very important in these reactions, and the shape of the potential energy surface (PES) has influence on the tunneling probability. Truong and co-workers[26] have calculated tunneling probabilities and rate constants for the double proton transfer in the water-assisted tautomerization, and found that tunneling effect is very large, which lowers the barrier about 4.6 kcal mol^{-1}. However, these theoretical studies are still for the gas phase, and no study has been performed for the

10.1021/jp983636+ CCC: $18.00
Published on Web 01/20/1999

solvent effect on the characteristics of the PES. Therefore, it is necessary to understand how solvation processes influence the PES. The characteristics of the PES, such as the tautomerization energy and the barrier for the double proton transfer, strongly depend on the level of the theoretical calculation, the size of the basis set ,and the inclusion of correlation energy. In this study, we investigated the solvent effect on the double proton transfer in the prototropic tautomerization of formamide, using the ab initio quantum mechanical calculations including the self-consistent reaction field.[27] Forming a homodimer can also facilitate the tautomerization reaction, and therefore we have studied the double proton transfer in the dimer-assisted as well as the water-assisted tautomerization in the gas phase and in solution. Since electron correlation plays an important role in determining the characteristics of the PES for the proton transfer reaction in the gas phase,[18,19,28−30] it is necessary to consider the correlation effect in solution too. The density functional theory has been successfully applied to the proton transfer reactions and it agrees well with other methods including high-level electron correlation. Recently Ruiz-López et al. have studied solvent effects on the proton transfer using density function theory including the self-consistent Onsager reaction field and they showed that the solute's correlation energy could be greatly modified in the solvation process.[31] We have also performed density functional theory calculations to investigate the change in the PES, compared with the Hartree−Fock (HF) level of calculation without the correlation effect, in the gas phase and in solution.

Computational Methods

All electronic structure calculations were done using the Gaussian 94 quantum mechanical packages.[32] Geometries for formamide (F), formamidic acid (FA), monohydrated formamide (FW), monohydrated formamidic acid (FAW), formamide dimer (FD), formamidic acid dimer (FAD), and the transition states (FWTS and FDTS) for the double proton transfer in the dimer-assisted and the water-assisted tautomerization were optimized at the Hartree−Fock (HF) level of theory using 6-31G(d,p), 6-31+G(d,p), 6-311G(d,p), and Dunning's correlation consistent double-ζ basis sets[33−35] with diffuse functions (AUG-cc-pVDZ) in the gas phase. The second and fourth-order Møller−Plesset perturbation theory (MP2 and MP4) calculations and the coupled cluster calculations including up to triple excitation [CCSD-(T)] were performed to calculate the potential energy barrier for the double proton transfer using the structures optimized at the MP2/6-31G(d,p) level. Density functional theory calculations using Becke's three-parameter[36] gradient-corrected exchange functional with the Lee−Yang−Parr[37] gradient-corrected correlation (B3LYP) were also performed using the 6-31G(d,p) basis set.

The self-consistent reaction field theory[27] was used to optimize structures and to calculate energies for various dielectric constants. Frequencies were calculated for transition state structures. The imaginary frequency at the transition state has been monitored with the variation of the dielectric constant. In the reaction field theory, the solute in a cavity is surrounded by a polarizable medium with a dielectric constant. A dipole in the solute induces a dipole in the medium, and the electric field applied to the solute by the solvent dipole will interact with the solute dipole to produce net stabilization. The cavity radius is the adjustable parameters, and the choice of the radius has been discussed extensively.[27,38−40] In the Onsager model,[41] the radius was calculated from the molecular volume of the optimized structure in the gas phase, on the assumption that the structure is spherical, and added by 0.5 to consider the surrounding solvent molecules. In the isodensity polarized continuum model (IPCM), the cavity is defined as an isosurface of the electron density.[42] The isodensity surface is determined by an iterative process in which an SCF cycle is performed and converged using the current isodensity cavity. The resulting wave function is used to update the isodensity cavity, and this procedure is repeated until the cavity shape changes no longer upon completion of the SCF. However, the terms that couple the isodensity to the solute Hamiltonian are missing in this process. In the self-consistent isodensity polarized continuum model (SCIPCM), the SCF procedure solves for the electron density which minimizes the energy, including solvation energy that depends on the cavity which depends on the electron density again.[43] Therefore, the effects of solvation are folded into the iterative SCF calculation. The SCIPCM thus accounts for the full coupling between the cavity and the electron density and includes terms that the IPCM neglects. The HF and B3LYP levels of theory were employed to calculate the solvent effect using the SCIPCM with the isodensity value of 0.0004.

The formation energies for the H-bonded complexes, E_{HB}, were calculated from the difference in energies between the complex and two different monomers. These energies correspond to the H-bond strengths. The basis set superposition error (BSSE) may be important in the calculation of the formation energies.[44] The BSSE was corrected by the Boys and Bernardi counterpoise correction scheme[45]

$$\mathrm{BSSE} = [E_m(M_1) - E_d(M'_1)] + [E_m(M_2) - E_d(M'_2)] + E_{reorg} \quad (1)$$

$$E_{reorg} = [E_m(M'_1) - E_m(M_1)] + [E_m(M'_2) - E_m(M_2)] \quad (2)$$

where $E_m(M)$ and $E_d(M')$ are the energies of the monomer in its own basis set and in the basis set of the H-bonded complex, respectively, and M and M′ denote the optimized geometry of monomer and the geometry of the monomer in the optimized H-bonded complex, respectively. The reorganization energy (E_{reorg}), i.e., the energy associated with the transition from the optimized geometry of monomer to the geometry which the monomer has in the H-bonded complex, should be also included in the correction of the BSSE. The corrected formation energy is determined as follows:

$$E_{HB}(\mathrm{corr}) = E(D) - [E_m(M_1) + E_m(M_2)] + \mathrm{BSSE} \quad (3)$$

$$= E(D) - [E_d(M'_1) + E_d(M'_2)] + E_{reorg}$$

where $E(D)$ is the energy of H-bonded complex.

Results and Discussion

Water-Assisted Tautomerization. The gas phase geometries for formamide (F), monohydrated formamide (FW), monohydrated formamidic acid (FAW), and the transition state (FWTS) for the double proton transfer were optimized at the HF/6-31G-(d,p) and B3LYP/6-31G(d,p) levels. The geometric parameters are shown in Figure 1. The B3LYP level calculation predicts slightly larger bond lengths for all bonds except the hydrogen bonds in the structures of FW and FAW. The H-bond distances of $r(O_2-H_1)$ and $r(O_1-H_2)$ in FW are 1.977 and 1.907 Å at the B3LYP level. They are about 0.07 and 0.25 Å shorter than the corresponding values at the HF level and agree better with

TABLE 1: H-Bond Strengths (E_{HB}), Reaction Energies (ΔE_T), and Barrier Heights ($\Delta E^{\ddagger}$) for Water-Assisted Tautomerization in the Gas Phase[a]

	E_{HB}	ΔE_T	$\Delta E^{\ddagger}$	ref
HF/6-31G(d,p)	−9.65, −9.41[b] (−6.84)[b]	11.6(12.3)	36.3(32.7)	this study
HF/cc-pVDZ		10.9(11.9)	35.4(32.0)	24
B3LYP/6-31G(d,p)	−13.5, −12.9[b] (−9.75)[b]	10.1(10.6)	19.5(16.2)	this study
BH&H-LYP/6-31G(d,p)	−13.2(−10.1)	10.5(11.0)	24.1(20.5)	26
BLYP/6-31G(d,p)	−13.7(−10.6)	9.8(10.1)	16.9(13.7)	26
MP2/cc-pVDZ	−12.8(−9.7)	9.22(10.2)	18.9(15.5)	24
QCISD/6-31G(d,p)		10.5	25.9	26
CISD(Full)/cc-pVDZ		9.60(10.6)	26.0(22.6)	24

[a] Energies are in kcal mol-1. Numbers in parentheses are with zero-point energies. The zero-point energies at the HF and the MP2 levels were weighted to 0.9 and 0.95, respectively. [b] The BSSEs are corrected.

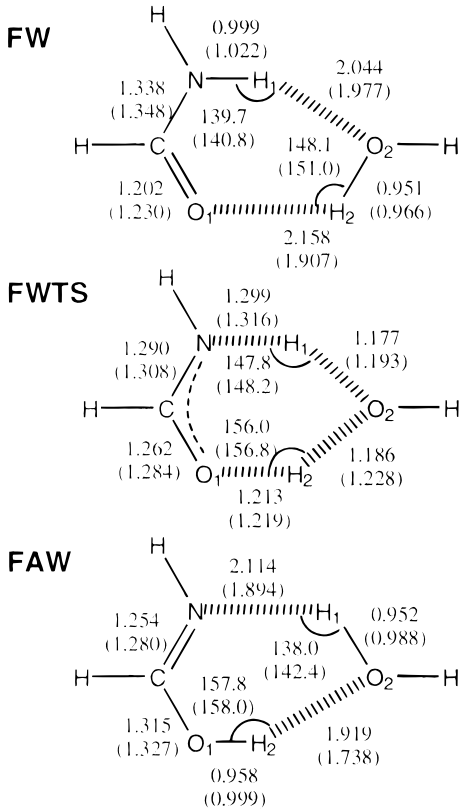

Figure 1. Geometric parameters of monohydrated formamide (FW), transition state (FWTS), and monohydrated formamidic acid (FAW) in the water-assisted prototropic tautomerism of formamide optimized at the HF/6-31G(d,p) and B3LYP/6-31G(d,p) levels in the gas phase. Numbers in parentheses are from the B3LYP calculation. Bond lengths are in Å, angles in degrees.

the high-level ab initio results including electron correlation.[24,26] The $r(N-H_1)$ and $r(O_2-H_2)$ values in the structure of FAW are larger at the B3LYP level but smaller at the HF level than the corresponding high-level ab initio results. However, the absolute magnitudes of their differences from the high-level ab initio results are approximately the same. Recently, the geometries for formic acid dimer[22] and monohydrated formamidine[46] have been calculated at the B3LYP/6-31G(d,p) level of theory. The H-bond distances in the formic acid dimer and in monohydrated formamidine are slightly smaller than the experimental and the high-level ab initio results including electron correlation, respectively. These results suggest that the B3LYP level of theory overestimates the strength of hydrogen bonds, which produces slightly short H bonds. The geometry of FWTS from the B3LYP method agrees better with the high-level ab initio results.[24,26] The double proton transfer in the water-assisted

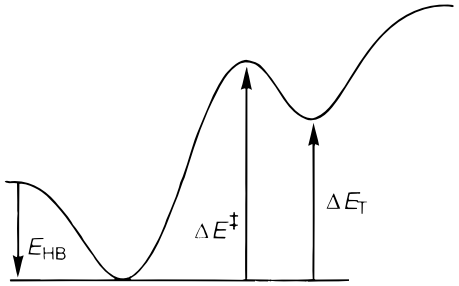

Figure 2. Schematic diagram for the energetics of the double proton transfer in prototropic tautomerizm of formamide.

tautomerization of formamide proceeds through a concerted mechanism in the gas phase, which agrees well with previous studies.[24,26]

Figure 2 shows the schematic diagram of energetic parameters for the protopropic tautomerism of formamide. The H-bond strengths (E_{HB}), tautomerization energies (ΔE_T), and barrier heights ($\Delta E^{\ddagger}$) in the gas phase are listed in Table 1. Simons and co-workers[24,26] have pointed out that the potential energy barrier for the tautomerization of formamide is 51.9 kcal mol^{-1} at the CISD(Full) level in the gas phase, and this is lowered by about 26 kcal mol^{-1} when a single water molecule is added. They have also shown that the tautomerization energy is 11.4 kcal mol^{-1} at the CISD(Full) level, and this value is lowered to 9.60 kcal mol^{-1} by adding a single water molecule. The tautomerization energy depends on the relative stability of two tautomers, FA and F, which is not changed much by adding a water molecule. The H bonds with a water molecule in FAW are slightly stronger than in FW,[26] which stabilize the energy of FAW more to reduce the tautomerization energy. The potential energy barrier is overestimated about 10 kcal mol^{-1} at the HF/6-31G(d,p) level but underestimated about 6 kcal mol^{-1} at the B3LYP/6-31G(d,p) level compared with the CISD(Full) value in the gas phase.

The geometries for F, FW, and FWTS in solution were optimized at the HF and B3LYP levels using the SCRF method. The geometric parameters in a medium of $\epsilon = 78.4$ are listed in Table 2. The $r(O_2-H_1)$ values in FW at the HF and B3LYP levels are 0.43 and 0.2 Å larger, respectively, than the corresponding values in the gas phase, while the $r(O_1-H_2)$ values at the HF and B3LYP levels are about 0.2 and 0.08 Å smaller, respectively. The partial charges of O_1 and N in the formamide moiety of FW were calculated at the HF level using the Mulliken population analysis, and they are −0.61 and −0.74 in the gas phase, and −0.64 and −0.73 in a dielectric medium of $\epsilon = 78.4$, respectively. These partial charges were also calculated using the natural population analysis (NPA), and they are −0.75 and −0.94 in the gas phase, and −0.77 and −0.93

TABLE 2: Geometric Parameters for Monohydrated Formamide at the HF and B3LYP Levels in a Dielectric Medium[a]

	HF		B3LYP	
	$\epsilon = 78.4$[b]	Δ[c]	$\epsilon = 78.4$	Δ
(A) Geometric Parameters for FW				
$r(C-O_1)$	1.207	0.005	1.236	0.006
$r(C-N)$	1.334	−0.004	1.343	−0.005
$r(N-H_1)$	0.996	−0.003	1.016	−0.006
$r(O_2-H_1)$	2.477	0.430	2.172	0.195
$r(O_2-H_2)$	0.952	0.001	0.984	0.018
$r(O_1-H_2)$	1.961	−0.197	1.827	−0.080
$\angle(N-H_1-O_2)$	132.6	−7.1	135.6	−5.2
$\angle(O_1-H_2-O_2)$	159.6	11.5	160.1	9.1
(B) Geometric Parameters for FAW				
$r(C-O_1)$	1.319	0.004	1.331	0.004
$r(C-N)$	1.253	−0.001	1.278	−0.002
$r(N-H_1)$	2.079	−0.035	1.872	−0.022
$r(O_2-H_1)$	0.954	0.002	0.990	0.002
$r(O_2-H_2)$	1.959	0.040	1.760	0.022
$r(O_1-H_2)$	0.956	−0.002	0.996	0.003
$\angle(N-H_1-O_2)$	141.0	3.0	143.8	1.4
$\angle(O_1-H_2-O_2)$	157.3	−0.5	157.9	−0.1
(C) Geometric Parameters for FWTS				
$r(C-O_1)$	1.278	0.016	1.293	0.009
$r(C-N)$	1.280	−0.010	1.303	−0.005
$r(N-H_1)$	1.167	−0.132	1.287	−0.029
$r(O_2-H_1)$	1.336	0.159	1.224	0.031
$r(O_2-H_2)$	1.438	0.251	1.281	0.053
$r(O_1-H_2)$	1.045	−0.168	1.172	−0.047
$\angle(N-H_1-O_2)$	150.0	2.1	149.1	0.9
$\angle(O_1-H_2-O_2)$	156.1	0.1	157.8	1.0

[a] Numbers in lengths and angles are correlated with the geometric parameters in Figure 1. Lengths in Å and angles in degrees. [b] Dielectric constant. [c] Deviations from the gas-phase geometries.

in a dielectric medium of $\epsilon = 78.4$, respectively. The larger negative charge on O_1 in solution makes the involving H bond stronger, so the $r(O_1-H_2)$ value becomes smaller, while the smaller negative charge on N makes the involving H bond weaker and the $r(O_2-H_1)$ value larger. The Mulliken charges on O_1 and N calculated at the B3LYP level are −0.49 and −0.58 in the gas phase, and −0.52 and −0.57 in a medium of $\epsilon = 78.4$, respectively, and the NPA charges are −0.65 and −0.87 in the gas phase, and −0.67 and −0.85 in a medium of $\epsilon = 78.4$, respectively. The changes in partial charges and the H-bond distances depending on the medium correlate well with those from the HF method. The $r(C-O_1)$ value becomes shorter, but the $r(C-N)$ value larger as the dielectric constant is increased at both the HF and B3LYP levels. These results suggest that the *enolate* form of the resonance structure of formamide becomes more favorable in a polar medium than in the gas phase. The $r(N-H_1)$ values in FAW at the HF and B3LYP levels are 0.035 and 0.022 Å smaller, while the $r(O_2-H_2)$ values are about 0.04 and 0.022 Å larger, respectively, in a medium of $\epsilon = 78.4$. In polar solution, the $r(C-O_1)$ value becomes shorter and the $r(C-N)$ value larger, as do the corresponding values in the formamide moiety of FW. The larger electron density on N of the formamidic acid moiety in FAW is supposed to make the hydrogen bond stronger and shorter. For the structure of FWTS, the H bonds to oxygen of water as a hydrogen-bond acceptor become longer with increasing the dielectric constant at both the HF and B3LYP levels. The values of $r(O_2-H_1)$ and $r(O_2-H_2)$ at the HF level are increased by about 0.16 and 0.25 Å, while the values of $r(N-H_1)$ and $r(O_1-H_2)$ decreased by about 0.13 and 0.17 Å, respectively, in a medium with $\epsilon = 78.4$. These changes in the H-bond lengths result in the separation of the partial charges

TABLE 3: Calculated H-Bond Strengths, Water-Assisted Tautomerization Energies, Barrier Heights, and Imaginary Frequencies in the Gas Phase and in Solution at the HF Level Using the Onsager SCRF Method[a]

ϵ[b]	E_{HB}[c]	ΔE_T[d]	$\Delta E^{\ddagger}$	$\nu^{\ddagger}$
gas	−9.65(−7.41)	11.6	36.3	2105i
2.0	−8.11(−5.63)	12.1	36.4	2053i
5.0	−7.01(−4.40)	12.7	36.1	1704i
10.0	−6.64(−4.01)	13.1	36.0	1571i
20.0	−6.47(−3.85)	13.3	35.9	1507i
40.0	−6.40(−3.79)	13.4	35.8	1507i
78.4	−6.35(−3.75)	13.5	35.8	1454i

[a] Energies in kcal mol^{-1} and frequencies in cm^{-1}. [b] Dielectric constants. [c] The H-bond strengths. Numbers in parentheses are the BSSE-corrected H-bond strengths. [d] The tautomerization energies.

TABLE 4: Calculated H-Bond Strengths, Water-Assisted Tautomerization Energies, Barrier Heights, and Imaginary Frequencies in the Gas Phase and in Solution at the B3LYP Level Using the Onsager SCRF Method[a]

ϵ[b]	E_{HB}[c]	ΔE_T[d]	$\Delta E^{\ddagger}$	$\nu^{\ddagger}$
gas	−13.5(−9.06)	10.1	19.5	1553i
2.0	−12.3(−7.59)	10.8	19.8	1559i
5.0	−11.4(−6.52)	11.6	20.3	1559i
10.0	−11.1(−6.18)	12.1	20.6	1552i
20.0	−11.0(−6.02)	12.3	20.7	1547i
40.0	−10.9(−5.95)	12.5	20.8	1545i
78.4	−10.9(−5.92)	12.6	20.9	1545i

[a] Energies in kcal mol^{-1} and frequencies in cm^{-1}. [b] Dielectric constants. [c] The H-bond strengths. Numbers in parentheses are the BSSE-corrected H-bond strengths. [d] The tautomerization energies.

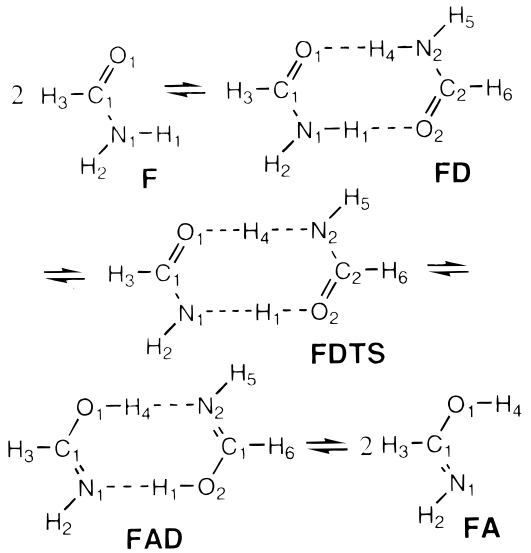

Figure 3. Schematic reaction diagram for the double proton transfer in the dimer-assisted prototropic tautomerism of formamide.

of FWTS to increase the dipole moment. The NPA charge of O_2-H moiety of FWTS calculated at the HF level is −0.56 in the gas phase and −0.71 in a medium of $\epsilon = 78.4$. The FWTS structure in a polar solvent has more ion-pair character than in the gas phase. The results from the B3LYP method are consistent with the HF results, although the changes in the H-bond lengths are smaller. The NPA charges of O_2-H moiety at the B3LYP level in the gas phase and in a medium of $\epsilon = 78.4$ are −0.51 and −0.54, respectively.

The values of E_{HB}, ΔE_T, $\Delta E^{\ddagger}$, and imaginary frequencies ($\nu^{\ddagger}$) in solution have been calculated at the HF level using the SCRF method, and the results are listed in Table 3. The BSSE-corrected H-bond strength in the gas phase is about 7.4 kcal mol^{-1}, and it is weakened as the dielectric constant is increased.

TABLE 5: Geometric Parameters for F, FA, FD, FAD, and FDTS at the HF, MP2, and B3LYP Levels Using Various Basis Sets[a]

(A) Geometric Parameters for F

	HF/6-31G(d,p)	B3LYP/6-31G(d,p)	MP2/6-31G(d,p)	expt
$r(C_1-N_1)$	1.348	1.361	1.361	1.352
$r(C_1-O_1)$	1.193	1.216	1.224	1.219
$r(C_1-H_3)$	1.092	1.109	1.101	1.098
$r(N_1-H_2)$	0.991	1.007	1.003	1.002
$r(N_1-H_1)$	0.994	1.009	1.006	1.002
$\angle(C_1-N_1-H_2)$	121.6	121.7	121.7	120.0
$\angle(C_1-N_1-H_1)$	119.0	118.9	118.8	118.5
$\angle(N_1-C_1-O_1)$	124.9	124.9	124.7	124.7
$\angle(N_1-C_1-H_3)$	112.8	112.0	112.2	112.7

(B) Geometric Parameters for FA

	HF/6-31G(d,p)	B3LYP/6-31G(d,p)	MP2/6-31G(d,p)
$r(C_1-N_1)$	1.246	1.267	1.275
$r(C_1-O_1)$	1.328	1.347	1.351
$r(C_1-H_3)$	1.081	1.094	1.088
$r(N_1-H_2)$	1.001	1.019	1.017
$r(O_1-H_4)$	0.948	0.973	0.971
$\angle(C_1-N_1-H_2)$	111.7	111.8	109.9
$\angle(C_1-O_1-H_4)$	108.3	106.1	105.4
$\angle(N_1-C_1-O_1)$	122.6	122.0	121.6
$\angle(N_1-C_1-H_3)$	126.7	128.0	128.1

(C) Geometric Parameters for FD[b]

	HF/6-31G(d,p)	HF/6-31+G(d,p)	HF/AUG-cc-pVDZ	B3LYP/6-31G(d,p)	MP2/6-31G(d,p)
$r(C_1-N_1)$	1.332	1.333	1.335	1.342	1.343
$r(C_1-O_1)$	1.205	1.207	1.206	1.232	1.238
$r(N_1-H_1)$	1.004	1.004	1.005	1.029	1.021
$r(O_1-H_4)$	1.999	2.017	2.011	1.850	1.886
$\angle(O_1-C_1-N_1)$	125.6	125.2	125.3	125.7	125.6
$\angle(C_1-N_1-H_1)$	120.3	120.2	120.3	120.7	120.5
$\angle(C_1-O_1-H_4)$	122.7	125.7	124.7	119.5	118.9
$\angle(N_1-H_1-O_2)$	171.5	169.0	169.7	174.1	175.0

(D) Geometric parameters for FAD[c]

	HF/6-31G(d,p)	HF/6-31+G(d,p)	HF/AUG-cc-pVDZ	B3LYP/6-31G(d,p)	MP2/6-31G(d,p)
$r(C_1-N_1)$	1.258	1.260	1.262	1.288	1.289
$r(C_1-O_1)$	1.304	1.305	1.309	1.306	1.317
$r(N_1-H_1)$	1.850	1.866	1.871	1.578	1.659
$r(O_1-H_4)$	0.970	0.969	0.968	1.043	1.017
$\angle(O_1-C_1-N_1)$	124.5	124.3	124.3	124.8	124.3
$\angle(C_1-N_1-H_1)$	125.5	125.5	125.4	125.0	126.2
$\angle(C_1-O_1-H_4)$	111.7	112.1	111.5	111.2	109.8
$\angle(N_1-H_1-O_2)$	178.3	178.1	178.8	178.7	179.7

(E) Geometric Parameters for the FDTS[d]

	HF/6-31G(d,p)	HF/6-31+G(d,p)	HF/AUG-cc-pVDZ	B3LYP/6-31G(d,p)	MP2/6-31G(d,p)
$r(C_1-N_1)$	1.286	1.284	1.284	1.298	1.303
$r(C_1-O_1)$	1.260	1.257	1.257	1.289	1.291
$r(N_1-H_1)$	1.377	1.420	1.426	1.394	1.354
$r(O_1-H_4)$	1.205	1.238	1.238	1.125	1.142
$r(C_2-N_2)$	1.283	1.284	1.284	1.298	1.303
$r(C_2-O_2)$	1.263	1.257	1.257	1.289	1.291
$r(N_2-H_4)$	1.256	1.268	1.268	1.394	1.354
$r(O_2-H_1)$	1.109	1.086	1.079	1.125	1.142
$\angle(O_1-C_1-N_1)$	125.0	125.0	125.0	125.1	124.9
$\angle(C_1-N_1-H_1)$	122.8	123.1	123.1	124.0	124.3
$\angle(C_1-O_1-H_4)$	114.5	114.4	114.4	112.3	111.4
$\angle(N_1-H_1-O_2)$	177.0	177.3	177.3	178.7	179.4
$\angle(O_2-C_2-N_2)$	125.0	125.0	125.0	125.1	124.9
$\angle(C_2-N_2-H_4)$	122.8	122.7	122.7	124.0	124.3
$\angle(C_2-O_2-H_1)$	114.5	114.6	114.6	112.3	111.4
$\angle(N_2-H_4-O_1)$	178.1	177.8	177.8	178.7	179.4

[a] Lengths are in Å and angles in degrees. [b] Formamide dimer has C_{2h} symmetry. [c] Formamidic acid dimer has C_{2h} symmetry. [d] The transition state structure at the HF level has C_s symmetry, but C_{2h} symmetry at both the B3LYP and MP2 levels.

It is about 3.8 kcal mol^{-1} at $\epsilon = 78.4$, which is still larger than general H-bond strength in aqueous solution. This discrepancy is attributed to the specific interactions in water such that the extra H bonds with bulk water interfere the hydrogen bonds between two constituents in the complex. The BSSE is 2.24 kcal mol^{-1} in the gas phase, and it is increased to 2.61 at $\epsilon =$

5. There is almost no change between $\epsilon = 5$ and 78.4. Interestingly, the BSSE does not depend much on the solvent effect. The value of ΔE_T is 11.6 kcal mol^{-1} in the gas phase, and increased to 13.5 kcal mol^{-1} at $\epsilon = 78.4$. The barrier of the double proton transfer in the gas phase is about 36 kcal mol^{-1}, which is very high compared with the CISD(full) results. This value is reduced in a polar medium, although the change is very small, only about 1.5 kcal mol^{-1} at $\epsilon = 78.4$. The B3LYP calculations were also performed for the solvent effect, and the results are listed in Table 4. The BSSE-corrected values of E_{HB} in the gas phase and in a medium of $\epsilon = 78.4$ are -9.06 and -5.92 kcal mol^{-1}, respectively. This means that the H-bond strength at $\epsilon = 78.4$ is 5.92 kcal mol^{-1}, which is even 2 kcal mol^{-1} larger than the HF result. This result suggests again that the B3LYP method might overestimate the H-bond strength. The BSSE at the B3LYP level is larger than at the HF level. The value of ΔE_T is about 10.1 kcal mol^{-1} in the gas phase, which agrees very well with the high-level ab initio results. This value is only 0.5 kcal mol^{-1} larger than the CISD(full) result, and increased by about 2.5 kcal mol^{-1} at $\epsilon = 78.4$. The potential energy barrier in the gas phase is about 19.5 kcal mol^{-1}. The B3LYP method underestimates the barrier height, but the value from the B3LYP method agrees better with the CISD result. This barrier is increased with the dielectric constant of medium, which is opposite to the HF results, but the change at $\epsilon = 78.4$ is only about 1.4 kcal mol^{-1}. These results suggest that the water-assisted tautomerization is not facilitated by providing polar environments. The single water molecule reduces the barrier height for the double proton transfer to assist the tautomerization of formamide; however, the polar medium tends to rather increase the barrier height and the reaction energy of the water-assisted tautomerization.

Dimer-Assisted Tautomerization. The geometries for formamide (F), formamidic acid (FA), formamide dimer (FD), formamidic acid dimer (FAD), and the transition state (FDTS) for the double proton transfer are optimized in the gas phase at the HF, MP2, and B3LYPlevels of theory. Two protons are transferred concertedly without high-energy intermediate, and Figure 3 shows the schematic reaction diagram for the double proton transfer in the dimer-assisted prototropic tautomerization of formamide. The geometric parameters for F, FA, FD, FAD, and FDTS are listed in Table 5. The geometric parameters for F agree well with experiments at all levels of calculation performed in this study with 6-31G(d,p) basis set. For both F and FA, the calculated bond lengths for C_1-N_1 and C_1-O_1 at the HF level are slightly shorter than the corresponding values at the B3LYP and the MP2 levels, but other bond lengths and angles are quite similar. The H-bond lengths of FD, $r(O_1-H_4)$, at the HF, B3LYP, and MP2 levels are about 2.0, 1.85, 1.89 Å, respectively. They agree very well with experiments.[47] The H-bond length of FAD, $r(N_1-H_1)$, at the HF/AUG-cc-pVDZ level is 1.87 Å, which agrees well with experimental result for similar type of H bonds i.e., 1.8 Å.[47] However, the values of $r(N_1-H_1)$ at the MP2 and the B3LYP levels are 1.66 and 1.58 Å, respectively. They are shorter than experimental results. The MP2 and the B3LYP levels of theory seem to predict short hydrogen bonds when the nitrogen of imines is a hydrogen-bond acceptor. The geometric parameters at the HF level using the AUG-cc-pVDZ and the 6-31+G(d,p) basis sets are quite similar. The transition state structure depends very much on the levels of calculation. All HF level calculations predict that the structure of FDTS has C_s symmetry. In the FDTS structure from the HF/6-31G(d,p) method, the values of $r(N_1-H_1)$, $r(N_2-H_4)$, $r(O_1-H_4)$, and $r(O_2-H_1)$ are 1.377, 1.256, 1.205, and 1.109 Å, respectively. The H_1 proton attached initially on N_1 is already transferred to O_2, and the second proton, H_4, is between O_1 and N_2. This indicates that the first proton moves earlier than the second as the reaction proceeds, and thus two protons are transferred asynchronously. To test whether there is any high-energy intermediate along the reaction coordinate, we have calculated the intrinsic reaction path for the double proton transfer starting from the transition state at the HF/6-31G(d,p) level, and the results are shown in Figure 4. There is no intermediate along the intrinsic reaction path, and the reaction proceeds smoothly from reactant to product. This suggests that, at the HF level of theory, the two protons are transferred concertedly but asynchronously. However, the MP2 and B3LYP levels predict that the structure of FDTS has C_{2h} symmetry. The values of $r(N_1-H_1)$ and $r(N_2-H_4)$ are the same, and so are the values of $r(O_1-H_4)$ and $r(O_2-H_1)$. These results suggest that the double proton transfer occurs concertedly and synchronously. The positions of two protons at the transition state are both closer to the oxygen atoms, which means that the transition state is late. This is reasonable since the tautomerization is endoergic.

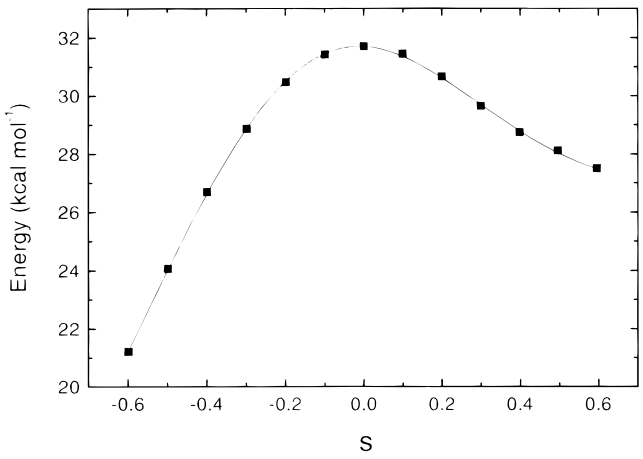

Figure 4. Intrinsic reaction path for double proton transfer in the dimer-assisted tautomerization calculated at the HF/6-31G(d,p) level. The horizontal axis is for the reaction coordinate in the unit of bohr, and the vertical axis for the relative energy of FDTS in terms of FD.

The energetic parameters such as E_{HB}, ΔE_T, and $\Delta E^{\ddagger}$ have been calculated in the gas phase at the HF, B3LYP, MP2, MP4, and the CCSD(T) levels. Imaginary frequencies for FDTS were also calculated, and the results are listed in Table 6. The calculated E_{HB} values depend on not only the electron correlation but also the BSSE. The values of E_{HB} for FD are -14.0 and -17.1 kcal mol^{-1} at the CCSD(T) level with and without zero-point energies, respectively. The E_{HB} values at the MP2 and the B3LYP levels agree very well with the CCSD(T) results, but all values at the HF levels are larger (H bonds are weaker). The BSSEs in the E_{HB} values at the MP2 and the B3LYP levels are about 3 kcal mol^{-1}. If we assume that the BSSE at the CCSD(T) level is the same, the H-bond strength for FD will be about 11 kcal mol^{-1}. The E_{HB} values for FAD are -19.2 and -20.8 kcal mol^{-1} at the CCSD(T) level with and without zero-point energies, respectively. They are -20.8 and -22.4 kcal mol^{-1} at the MP2 level, and -23.5 and -24.4 kcal mol^{-1} at the B3LYP level, respectively. The B3LYP level of theory slightly overestimates the H-bond strength of FAD, which makes short H bonds as listed in Table 5. The BSSEs at the MP2 and B3LYP levels are slightly larger than at the HF level. The HF level of calculation with Dunning's AUG-cc-pVDZ basis set has very small BSSEs in this study, which are 0.5 and 0.7 kcal mol^{-1} for the E_{HB} values of FD and FAD, respectively.

TABLE 6: Calculated H-Bond Strengths for FD and FAD, Dimer-Assisted Tautomerization Energies, Barrier Heights, and Imaginary Frequencies in the Gas Phase[a]

	E_{HB}(FD)[b]	E_{HB}(FAD)[c]	ΔE_T	$\Delta E^{\ddagger}$	$\nu^{\ddagger}$ (cm^{-1})
HF/3-21G[d]	−22.8	−29.8	28.1	29.9	
HF/6-31G(d,p)	−13.4(−11.2)	−16.9(−15.0)	21.9[22.8]	31.7[27.6]	1663i
	[−10.8(−8.65)]	[−14.8(12.9)]			
HF/6-31+G(d,p)	−11.7(−11.2)	−15.2(−14.0)	22.1[23.1]	32.6[28.7]	1726i
	[−9.43(−8.88)]	[−13.1(−11.9)]			
HF/6-311G(d,p)	−12.7(−10.5)	−16.3(−13.9)	21.4[22.6]	32.7[28.5]	1734i
	[−10.2(−8.02)]	[−14.2(−11.7)]			
HF/AUG-cc-pVDZ	−11.3(−10.8)	−13.9(−13.2)	20.9[22.0]	32.0[28.3]	1722i
	[−8.88(−8.33)]	[−11.7(−11.0)]			
B3LYP/6-31G(d,p)	−17.4(−14.4)	−24.4(−20.8)	18.3[17.7]	18.8[15.3]	703i
	[−14.8(−11.7)]	[−23.5(−19.8)]			
MP2/6-31G(d,p)	−17.2(−14.0)	−22.4(−17.3)	19.4[19.3]	21.3[17.6]	1097i
	[−14.1(−10.9)]	[−20.8(−15.7)]			
MP4//MP2/6-31G(d,p)	−17.1[−14.1][e]	−21.5[−19.8][e]	19.7[19.5][e]	22.5[18.6][e]	
CCSD(T)//MP2/6-31G(d,p)	−17.1[−14.0][e]	−20.8[−19.2][e]	18.0[17.9][e]	21.6[17.7][e]	

[a] Energies are in kcal mol^{-1}. Numbers in brackets are with zero-point energies. Numbers in parentheses are the BSSE-corrected H-bond strengths. The zero-point energies at the HF and the MP2 levels were weighted to 0.9 and 0.95, respectively. [b] The H-bond strength of FD calculated from the energy difference between FD and two F molecules. [c] The H-bond strength of FAD calculated from the energy difference between FAD and two F molecules. [d] Reference 23 [e] The zero-point energies at the MP2 level were used.

The energetic parameters depend on the levels of theory and the size of the basis sets very much. When we consider the electron correlation with the MP2 method, the tautomerization energy and the potential energy barrier are reduced by about 2.5 and 10 kcal mol^{-1}, respectively. The potential energy barrier for the double proton transfer is very sensitive to the electron correlation, which is consistent with previous studies.[15,46] The imaginary frequencies calculated at the HF level are all larger than those at the MP2 and B3LYP levels. The dimer-assisted tautomerization is very endoergic. The values of ΔE_T and $\Delta E^{\ddagger}$ were calculated at the CCSD(T) level, and they are 18.0 and 21.6 kcal mol^{-1}, respectively. The potential energy barrier for the tautomerization is lowered about 30 kcal mol^{-1} in the gas phase by forming hydrogen-bonded dimer. The ΔE_T value for the dimer-assisted tautomerization is almost twice the value for the water-assisted tautomerization. Since the tautomerization energy of the single formamide is 11.4 kcal mol^{-1} at the CISD-(Full) level[24] and there are two formamide molecules in the dimer, the reaction energy for dimer-assisted tautomerization would be 22.8 kcal mol^{-1} if there is no energetic contribution from the H bonds. The tautomerization energy at the CCSD(T) level is about 4.8 kcal mol^{-1} lower than this, and this stabilization originates from the relative H-bond strengths of FD and FAD as listed in Table 6. These results suggest that the tautomerization energy is entirely determined by the relative energies of tautomers and the relative H-bond strengths of FD and FAD. The single point calculation at the MP4//MP2/6-31G-(d,p) level slightly increases the values of ΔE_T and $\Delta E^{\ddagger}$ from the MP2 level, indicating that higher order Møller−Plesset perturbation terms do not seem to improve the results.

The H-bond strengths in solution were calculated at the HF/6-31G(d,p) and B3LYP/6-31G(d,p) levels using the Onsager SCRF method, and the results are listed in Table 7. The B3LYP method predicts stronger H-bonds for both FD and FAD. The values of E_{HB}(FD) at both HF and B3LYP levels are increased (the H bonds are weakened) with the dielectric constant. They are −6.67 and −11.2 kcal mol^{-1} at $\epsilon = 78.4$ without the BSSE correction, respectively. When the BSSEs are corrected these values become −4.21 and −6.70 kcal mol^{-1}, respectively. Although these H-bond strengths are reduced by about 7 kcal mol^{-1} compared with the corresponding gas phase values, they are still larger than the experimental values in aqueous solution. The BSSEs of E_{HB}(FD) at the HF and B3LYP levels are about 2.2−2.4 and 4.1−4.5 kcal mol^{-1}, respectively, and they are almost independent of the dielectric constant. The E_{HB}(FAD) values at both HF and B3LYP levels do not depend on the dielectric constant much, and the change is less than 1 kcal mol^{-1}. Since the H-bond strength of FD is reduced further than that of FAD as the dielectric constant is increased, the reaction energy of dimer-assisted tautomerization would be increased in a polar solvent. The tautomerization energies and the barrier height were calculated at the HF/6-31G(d,p) and B3LYP/6-31G-(d,p) levels using the SCIPCM. The global dipole moments of FD and FDTS are zero since they have C_{2h} symmetry, and this gives zero reaction field in the Onsager SCRF model using spherical cavity so that there would be no energetic stabilization. Therefore, the SCIPCM that uses the cavity defined by an isodensity surface coupled with the electron density of the molecule would be appropriate for the reasonable estimation for the solvation energy. The results are listed in Table 8. We have also calculated the E_{HB}(FD) values using the SCIPCM, which are −10.4, −7.87, −6.32, and −5.89 kcal mol^{-1} at the HF level, and −14.8, −12.5, −11.0, and −10.6 kcal mol^{-1} at the B3LYP level in a medium of $\epsilon = 2$, 5, 20, 78.4, respectively. When they are compared with the results from the Onsager SCRF model as shown in Table 7, the largest error is 0.8 kcal mol^{-1} for FD at the HF level, which is not very large. This suggests that the Onsager SCRF model can also give quite reasonable results for the solvation energy. The values of $\Delta E^{\ddagger}$ and ΔE_T at both the HF and the B3LYP levels are increased with the dielectric constant. The $\Delta E^{\ddagger}$ and ΔE_T values of $\epsilon =$

TABLE 7: Calculated H-Bond Strengths for FD and FAD in Solution at the HF/6-31G(d,p) and B3LYP/6-31G(d,p) Levels Using the Onsager SCRF Method[a]

	HF/6-31G(d,p)		B3LYP/6-31G(d,p)	
ϵ	E_{HB}(FD)[b]	E_{HB}(FAD)[c]	E_{HB}(FD)	E_{HB}(FAD)
gas	−13.4(−11.2)	−16.9(−15.0)	−17.4(−13.3)	−24.4(−20.8)
2	−10.8(−8.55)	−16.7(−14.7)	−15.1(−10.8)	−24.2(−20.5)
5	−8.57(−6.18)	−16.4(−14.4)	−13.0(−8.60)	−24.1(−20.3)
10	−7.61(−5.19)	−16.3(−14.3)	−12.1(−7.64)	−24.0(−20.2)
20	−7.06(−4.64)	−16.2(−14.2)	−11.6(−7.11)	−24.0(−20.1)
40	−6.81(−4.35)	−16.2(−14.1)	−11.3(−6.84)	−24.0(−20.1)
78.4	−6.67(−4.21)	−16.2(−14.1)	−11.2(−6.70)	−24.0(−20.1)

[a] Energies are in kcal mol^{-1}. Numbers in parentheses are the BSSE-corrected H-bond strengths. [b] The H-bond trength of FD calculated from the energy difference between FD and two F molecules. [c] The H-bond trength of FAD calculated from the energy difference between FAD and two F molecules.

TABLE 8: Calculated Barrier Heights and Dimer-Assisted Tautomerization Energies in Solution at the HF/6-31G(d,p) and B3LYP/6-31G(d,p) Levels Using the SCIPCM[a]

	HF/6-31G(d,p)		B3LYP/6-31G(d,p)	
ϵ	$\Delta E^{\ddagger b}$	$\Delta E_T{}^c$	$\Delta E^{\ddagger b}$	$\Delta E_T{}^c$
gas	31.7	21.9	18.8	18.3
2	32.4	23.2	19.6	19.3
5	33.0	24.4	20.4	20.1
20	33.3	25.2	20.7	20.7
78.4	33.4	25.5	21.0	20.8

[a] Energies are in kcal mol^{-1}. [b] Barrier height for the double proton transfer. [c] Tautomerization energies calculated from the differences in energy between FD and FAD.

78.4 are 1.8 and 3.6 kcal mol^{-1} larger at the HF level, and 2.2 and 2.5 kcal mol^{-1} larger at the B3LYP level, than the corresponding values in the gas phase. These results suggest that the dimer-assisted tautomerization of formamide become less favorable in a polar solvent.

Concluding Remarks

The double proton transfer in water-assisted tautomerization of formamide occurs concertedly both in the gas phase and in solution. The FWTS structure in a polar solvent has more ion-pair character than in the gas phase. The BSSEs in the values of E_{HB} for monohydrated formamide are small and almost independent of dielectric constant. The single water molecule reduces the barrier height for the double proton transfer to assist the tautomerization of formamide; however, the polar medium tends to rather increase the barrier height and the reaction energy of the water-assisted tautomerization. The double proton transfer in the dimer-assisted tautomerization occurs via a concerted mechanism both in the gas phase and in solution. At the HF level of theory, the transition state has C_s symmetry, which suggests that the double proton transfer occurs asynchronously. At the MP2 and the B2LYP levels of theory, however, the transition state has C_{2h} symmetry, which means that double proton transfer occurs concertedly and synchronously. The HF level predicts incorrect structure for the transition state. The symmetry of the transition state does not change with solvent. The potential energy barrier for the tautomerization is lowered by about 30 kcal mol^{-1} in the gas phase by forming hydrogen-bonded dimer. The ΔE_T value for the dimer-assisted tautomerization is almost twice the value for the water-assisted. This value is entirely determined by the relative energies between tautomers and the relative H-bond strengths. Since the energy of formamidic acid is much higher than of formamide and the H-bond strengths of FD and FAD are not different very much, the reaction energy of the dimer-assisted reaction is higher than that of the water-assisted. However, the potential energy barrier for the double proton transfer in the dimer-assisted reaction is about 4 kcal mol^{-1} lower than the barrier in the water-assisted. These results suggest that the dimer-assisted tautomerization is kinetically more favorable, but thermodynamically less favorable. The values of $\Delta E^{\ddagger}$ and ΔE_T at both the HF and the B3LYP levels are increased with the dielectric constant, and therefore the dimer-assisted tautomerization becomes less favorable in a polar solvent as well as the water-assisted reaction. The BSSEs of E_{HB} in formamide dimer are almost independent of the dielectric constant. Electron correlation turns out to be crucial to the PES for the double proton transfer in the gas phase and also in solution.

Acknowledgment. We acknowledge the financial support of the Korea Research Foundation in the program year of 1997.

References and Notes

(1) Bell, R. P. *The Tunnel Effect in Chemistry*; Chapman and Hall: New York, 1980.
(2) Melander, L.; Saunders: W. H. J. *Reaction Rates of Isotopic Molecules*; John Wiley and Sons: New York, 1980; p 152.
(3) Bender, M. L. *Mechanisms of Homogeneous Catalysis from Protons to Proteins*; John Wiley & Sons: New York, 1971, Chapters 2, 4, 5.
(4) Schlabach, M.; Limbach, H.-H.; Bunnenberg, E.; Shu, A. Y. L.; Tolf, B.-R.; Djerassi, C. *J. Am. Chem. Soc.* **1993**, *115*, 4554.
(5) Scherer, G.; Limbach, H.-H. *J. Am. Chem. Soc.* **1989**, *111*, 5946.
(6) Scherer, G.; Limbach, H.-H. *J. Am. Chem. Soc.* **1994**, *116*, 1230.
(7) Meschede, L.; Limbach, H.-H. *J. Phy. Chem.* **1991**, *95*, 10267.
(8) Gerritzen, D.; Limbach, H.-H. *J. Am. Chem. Soc.* **1984**, *106*, 869.
(9) Svensson, P.; Bergman, N.-Å.; Ahlberg, P. *J. Chem. Soc., Chem. Commun.* **1990**, 862.
(10) Chang, Y.-T.; Yamaguchi, Y.; Miller, W. H.; Schaefer III, H. F. *J. Am. Chem. Soc.* **1987**, *109*, 7245.
(11) Millikan, R. C.; Pitzer, K. S. *J. Am. Chem. Soc.* **1958**, *80*, 3515.
(12) Bertie, J. E.; Michaelian, K. H. *J. Chem. Phys.* **1982**, *76*, 886.
(13) Bertie, J. E.; Michaelian, K. H.; Eysel, H. H. *J. Chem. Phys.* **1986**, *85*, 4779.
(14) Shida, N.; Barbara, P. F.; Almlof, J. *J. Chem. Phys.* **1991**, *94*, 3633.
(15) Kim, Y. *J. Am. Chem. Soc.* **1996**, *118*, 1522.
(16) Hrouda, V.; Florian, J.; Polesek, M.; Hobza, P. *J. Phys. Chem.* **1994**, *98*, 4742.
(17) Hrouda, V.; Florian, J.; Hobza, P. *J. Phys. Chem.* **1993**, *97*, 1542.
(18) Svensson, P.; Bergman, N.- Å.; Ahlberg, P. *J. Chem. Soc., Chem. Commun.* **1990**, 82.
(19) Nguyen, K. A.; Gordon, M. S.; Truhlar, D. G. *J. Am. Chem. Soc.* **1991**, *113*, 1596.
(20) Bell, R. L.; Truong, T. N. *J. Chem. Phys.* **1994**, *101*, 10442.
(21) Kim, Y. *J. Phys. Chem. A* **1998**, *102*, 3025.
(22) Lim, J.-H.; Lee, E. K.; Kim, Y. *J. Phys. Chem.* **1997**, *101*, 2233.
(23) Zielinski, T. J.; Poirier, R. A. *J. Comput. Chem.* **1984**, *5*, 466.
(24) Wang, X.-C.; Nichols, J.; Feyereisen, M.; Gutowski, M.; Boatz, J.; Haymet, A. D. J.; Simons, J. *J. Phys. Chem.* **1991**, *95*, 10419.
(25) Schegel, H. B.; Gund, P.; Fluder, E. M. *J. Am. Chem. Soc.* **1982**, *104*, 5347.
(26) Bell, R. L.; Taveras, D. L.; Truong, T. N.; Simons, J. *Int. J. Quantum Chem.* **1997**, *63*, 861.
(27) Tapia, O. In *Molecular Interactions*; Ratajczak, H., Orville-Thomas, W. J., Eds.; Wiley: New York, 1982; Vol. 3, p 47.
(28) Luth, K.; Scheiner, S. *J. Chem. Phys.* **1992**, *97*, 7519.
(29) Latajka, Z.; Scheiner, S.; Chalasinski, G. *Chem. Phys. Lett.* **1992**, *196*, 384.
(30) Szczesniak, M. M.; Scheiner, S. *J. Chem. Phys.* **1986**, *84*, 6328.
(31) Ruiz-Lopez, M. F.; Bohr, F.; Martins-Costa, M. T. C.; Rinaldi, D. *Chem. Phys. Lett.* **1994**, *221*, 109.
(32) Frisch, M. J.; Trucks, G. W.; Schlegel, H. B.; Gill, P. M. W.; Johnson, B. G.; Robb, M. A.; Cheeseman, J. R.; Keith, T. A.; Petersson, G. A.; Montgomery, J. A.; Raghavachari, K.; Al-Laham, M. A.; Zakrzewski, V. G.; Ortiz, J. V.; Foresman, J. B.; Cioslowski, J.; Stefanov, B. B.; Nanayakkara, A.; Challacombe, M.; Peng, C. Y.; Ayala, P. Y.; Chen, W.; Wong, M. W.; Andres, J. L.; Replogle, E. S.; Gomperts, R.; Martin, R. L.; Fox, D. J.; Binkley, J. S.; Defrees, D. J.; Baker, J.; Stewart, J. P.; Head-Gordon, M.; Gonzalez, C.; Pople, J. A. *Gaussian 94*; Gaussian, Inc.: Pittsburgh, 1995.
(33) Dunning Jr, T. H. *J. Chem. Phys.* **1989**, *90*, 1007.
(34) Kendall, R. A.; Dunning Jr, T. H.; Harrison, R. J. *J. Chem. Phys.* **1992**, *96*, 6796.
(35) Woon, D. E.; Dunning Jr, T. H. *J. Chem. Phys.* **1993**, *98*, 1358.
(36) Becke, A. D. *J. Chem. Phys.* **1993**, *98*, 5648.
(37) Lee, C.; Yang, W.; Parr, R. G. *Phys. Rev. B* **1988**, 786.
(38) Wong, M. W.; Frisch, M. J.; Wiberg, K. B. *J. Am. Chem. Soc.* **1991**, *113*, 4776.
(39) Szafran, M.; Karelson, M. M.; Katritzky, A. R.; Koput, J.; Zerner, M. C. *J. Comput. Chem.* **1993**, *14*, 371.
(40) Rivail, J. L.; Terryn, B.; Rinaldi, D.; Ruiz-Lopez, M. F. *J. Mol. Struct.* **1985**, *120*, 387.
(41) Onsager, L. *J. Am. Chem. Soc.* **1936**, *58*, 1486.
(42) Foresman, J. B.; Keith, T. A.; Wiberg, K. B.; Snoonian, J.; Frisch, M. J. *J. Phys. Chem.* **1996**, *100*, 16098.
(43) Foresman, J. B.; Frisch, A. *Exploring Chemistry with Electronic Structure Methods*, 2nd ed.; Gaussian, Inc.: Pittsburgh, PA, 1996; p 237.
(44) Scheiner, S. In *Calculation the Properties of Hydrogen Bonds by ab initio Methods*; Lipkowitz, K. B., Boyd, D. B. Eds.; VCH: New York, 1991; Vol. 2, p 165.
(45) Boys, S. F.; Bernardi, F. *Mol. Phys.* **1970**, *19*, 553.
(46) Zhang, Q.; Bell, R.; Truong, T. N. *J. Phys. Chem.* **1995**, *99*, 592.
(47) Shimoni, L.; Glusker, J. P.; Bock, C. W. *J. Phys. Chem.* **1996**, *100*, 2957.